

Article

Wear Resistance Prediction of AlCoCrFeNi-X (Ti, Cu) High-Entropy Alloy Coatings Based on Machine Learning

Jiajie Kang ^{1,2} , Yi Niu ¹, Yongkuan Zhou ^{1,3,*} , Yunxiao Fan ^{1,*} and Guozheng Ma ⁴¹ School of Engineering and Technology, China University of Geosciences, Beijing 100083, China² Zhengzhou Institute, China University of Geosciences, Zhengzhou 451283, China³ School of Materials Science and Engineering, Jiangsu University of Science and Technology, Zhenjiang 212100, China⁴ National Key Lab for Remanufacturing, Academy of Armored Forces Engineering, Beijing 100072, China

* Correspondence: yongkuanz@163.com (Y.Z.); fanyxiao@cugb.edu.cn (Y.F.)

Abstract: In order to save the time and cost of friction and wear experiments, the coating composition (different contents of Al, Ti, and Cu elements), ratio of hardness and elastic modulus (H^3/E^2), vacuum heat treatment (VHT) temperature, and wear form were used as input variables, and the wear rates of high-entropy alloy (HEA) coatings were used as output variables. The dataset was entirely obtained by experiment. Four machine learning algorithms (classification and regression tree (CART), random forest (RF), gradient boosting decision tree (GBDT), and adaptive boosting (AdaBoost)) were used to predict the wear resistance of HEA coatings based on a small amount of data. The results show that except for the GBDT model, the other three models had good performance. Because of the small amount of data, the CART model demonstrated the best prediction performance and can provide guidance for predicting the wear resistance of AlCoCrFeNi-X (Ti, Cu) HEA coatings for drilling equipment. Furthermore, the contribution of different factors to the wear rate of AlCoCrFeNi-X (Ti, Cu) HEA coatings was obtained. Al content had the greatest influence on wear rate, followed by H^3/E^2 , wear form, and VHT temperature.

Keywords: high-entropy alloy coating; HVOF; wear; machine learning

Citation: Kang, J.; Niu, Y.; Zhou, Y.; Fan, Y.; Ma, G. Wear Resistance Prediction of AlCoCrFeNi-X (Ti, Cu) High-Entropy Alloy Coatings Based on Machine Learning. *Metals* **2023**, *13*, 939. <https://doi.org/10.3390/met13050939>

Academic Editor: João Manuel R. S. Tavares

Received: 3 April 2023

Revised: 2 May 2023

Accepted: 10 May 2023

Published: 11 May 2023



Copyright: © 2023 by the authors. Licensee MDPI, Basel, Switzerland. This article is an open access article distributed under the terms and conditions of the Creative Commons Attribution (CC BY) license (<https://creativecommons.org/licenses/by/4.0/>).

1. Introduction

Wear is a common form of part failure, and improving the wear resistance of materials can increase the service life of parts. Metallurgy, drilling, mining, electric power, water conservancy, and agricultural industries have high requirements for the wear resistance of mechanical equipment [1–3]. Research regarding high-entropy alloys (HEAs) has been widely concerned with four significant effects: the high-entropy effect, delayed diffusion effect, lattice distortion effect, and cocktail effect [4–6]. HEAs demonstrate greater strength, hardness, and wear resistance compared with traditional alloys [7,8]. Among the HEAs, the CoCrFeNi-based HEAs are the most widely studied [9,10]. Due to the larger atomic radius of Al, the lattice constant and deformation of high-entropy alloys will increase significantly with the addition of Al content, which will lead to changes in its phase microstructure and mechanical properties. In addition, increasing the Al content will cause solid solution strengthening by forming strong covalent bonds with neighboring atoms [11–13]. The specific strength of Ti is very high, the larger atomic radius can cause lattice distortion and achieve solid solution strengthening, and Ti has been proven to increase the hardness of HEAs [14]. Therefore, the addition of Ti is also expected to improve the wear resistance of HEAs. Pure copper has good plasticity, and the addition of Cu may lead HEAs to demonstrate better self-lubrication, thereby improving the tribological properties of HEAs [15].

The preparation of wear-resistant coatings is one of the methods used to enhance the wear resistance of the materials. Thermal spraying technology is a method that uses a heat

source to heat the spraying material to a molten or semi-molten state and then sprays a deposition material at a particular rate onto the pretreated substrate surface to form the coating. Thermal spraying techniques include flame spraying and plasma spraying, which are widely used in the preparation of wear-resistant HEA coatings [16,17]. Thermal-sprayed coatings often have defects such as local segregation, cracks, and pores. Heat treatment is a common post-treatment process for sprayed coatings. Appropriate heat treatment can effectively homogenize the microstructure of the coating, reduce component segregation, and improve the wear resistance of the coating [18,19].

Wear testing has a high cost and a long test time, and it requires special test equipment. Moreover, there are many factors affecting wear, such as material composition, preparation, hardness, surface roughness, wear parameters, etc. [20–24]. These factors often have nonlinear relationships. Machine learning has strong processing ability in dealing with nonlinear data and can be used to deal with complex data and analyze correlations; therefore, using machine learning algorithms to predict material wear is a potentially effective means which can greatly save test costs and time and improve research efficiency [25,26].

Studies have been carried out on machine learning algorithms for predicting material wear [27,28]. Ulas et al. [29] predicted the wear loss of plasma transfer arc welding coatings by using four different machine learning algorithms (artificial neural network, extreme learning machine, kernel-based extreme learning machine, and weighted extreme learning machine). These four machine learning algorithms predicted the amount of wear of different coatings. The weighted extreme learning machine learning algorithm showed the highest prediction accuracy for the wear loss of coatings. Altay et al. [30] predicted the wear amounts of ferro-alloy coatings by using different machine learning algorithms (linear regression and Gaussian process regression). The results show that these three machine learning models can effectively save test time and reduce friction and wear test costs. The Gaussian process regression algorithm demonstrated the best performance for predicting the wear loss of ferro-alloy coatings. A neural network algorithm was used to model the database by using coating microhardness, load, environment, and friction test duration as the input variables and wear amount as the output variable, and the predicted results were in good agreement with the experimental results [25]. A machine learning method (artificial neural network) was also used to predict the erosion wear rate of cermet coatings prepared by the high-velocity oxygen fuel and flame spray flexicord techniques [31].

AlCoCrFeNi-X (Ti, Cu) HEAs are a powerful candidate for wear-resistant materials, and wearable components in drilling equipment often require the preparation of wear-resistant coatings on their surfaces to improve their wear resistance. Therefore, HVOF-sprayed AlCoCrFeNi-X (Ti, Cu) HEA coatings are expected to be applied in drilling equipment. In the past, experimental methods were often used to analyze the amount of material wear, which cost a great deal of time and money. With the rise of computer science, machine learning technology was used to predict material wear. The machine learning methods selected in previous relevant studies often required large amounts of data, but the amount of data on material wear is often limited; thus, the accuracy of prediction was not high enough. Therefore, based on a limited dataset, this study adopts the classification and regression tree (CART) machine learning algorithm—compatible with limited datasets—and the derived algorithms (random forest (RF), gradient boosting decision tree (GBDT) and adaptive boosting (AdaBoost)) based on the CART algorithm to predict the wear rate of AlCoCrFeNi-X (Ti, Cu) HEA coatings in drilling equipment. It is hoped that an optimized model for predicting the wear-resistant AlCoCrFeNi-X (Ti, Cu) HEA coatings for drilling equipment will be obtained so as to improve the efficiency of scientific research and save costs.

2. Methodology

This study was mainly carried out in three steps, as shown in Figure 1. Step 1: determine the input variable and collect relevant data. Step 2: select and analyze the

machine learning models. Step 3: evaluate the performance of the machine learning models and analyze the feature importance of input variables.

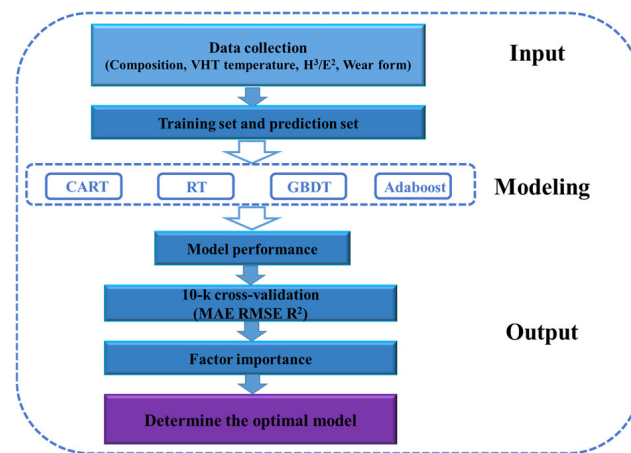


Figure 1. The analysis framework for machine learning.

2.1. Input Variable Determination and Data Collection

2.1.1. Input Variable Determination

The effect of composition (Al, Ti, and Cu) on the wear of AlCoCrFeNi-X (Ti, Cu) HEA coatings was explained in the introduction. The ratio of hardness and elastic modulus (H^3/E^2) can reflect the elastic strain and the resistance to plastic deformation of the coatings, and H^3/E^2 can reflect the wear resistance of the material [32]. The higher the ratio of H^3/E^2 , the better the wear resistance of the coating. Vacuum heat treatment (VHT) can improve the microstructure and mechanical properties of the coatings, but the mechanical properties of the coatings are different after VHT at different temperatures. Moreover, the wear of the coatings is affected by the wear form. Different wear forms (such as dry wear and wet wear) are very important to the wear rate of the coatings. Therefore, the input variables of the machine learning models were the coating composition (different contents of Al, Ti, and Cu elements), ratio of hardness and elastic modulus (H^3/E^2), VHT temperature, and wear form.

2.1.2. Data Collection

The dataset in this study was obtained entirely by experiments. HEA powders were prepared by vacuum atomization; according to atomic percentage, these can be expressed as Al_{0.4}CoCrFeNi, Al_{0.7}CoCrFeNi, AlCoCrFeNi, Al_{0.875}Ti_{0.125}CoCrFeNi, Al_{0.75}Ti_{0.25}CoCrFeNi, and AlCoCrFeNiCu, and the six mixture powders were denoted as 1, 2, 3, 4, 5, and 6, respectively. The coatings were prepared on an AISI 4135 steel (a common material used in drilling equipment) substrate by HVOF technology (GTV MF-P-HVF-FP-K 2000 HVOF system). The flow rates of N₂, H₂, and O₂ were 20, 580, and 190 slpm, respectively. The powder feed rate was 40 g/min and the spray distance was 230 mm. The microstructure of HVOF-sprayed AlCoCrFeNi-X (Ti, Cu) HEA coatings is shown in Figure 2. The coating was well combined with the substrate, and there were few pores and local segregation.

Then, the sprayed coating was subjected to VHT at different temperatures (500, 700, and 900 °C) for 4 h. The AlCoCrFeNi-X (Ti, Cu) HEA coatings subjected to different temperature VHT were sorted by composition, and the 24 coatings were labeled 1, 2, . . . , 24, respectively. A nano-indentation test was carried out using a nano-indenter (AGILENT U9820A, Nano Indenter G200, KLA-Tencor, Milpitas, CA, USA) with a maximum load of 10 mN and a holding time of 20 s. Each sample used for nano-indentation test was tested 5 times. The nano hardness and elastic modulus of the coating were obtained through the nano-indentation test. Figure 3 shows the ratio of hardness to elastic modulus (H^3/E^2) of the HEA coatings.

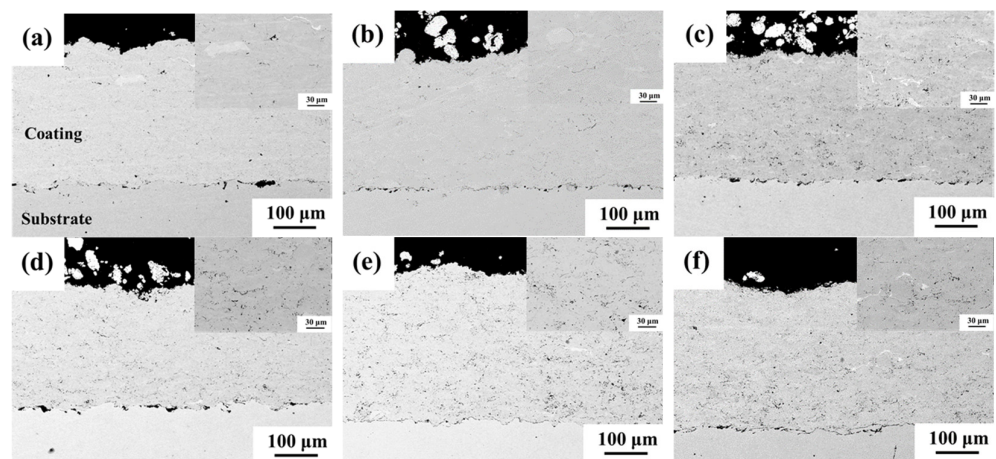


Figure 2. Microstructure of HVOF-sprayed AlCoCrFeNi-X (Ti, Cu) HEA coatings. (a) Al_{0.4}CoCrFeNi; (b) Al_{0.7}CoCrFeNi; (c) AlCoCrFeNi; (d) Al_{0.875}Ti_{0.125}CoCrFeNi; (e) Al_{0.75}Ti_{0.25}CoCrFeNi; and (f) AlCoCrFeNiCu.

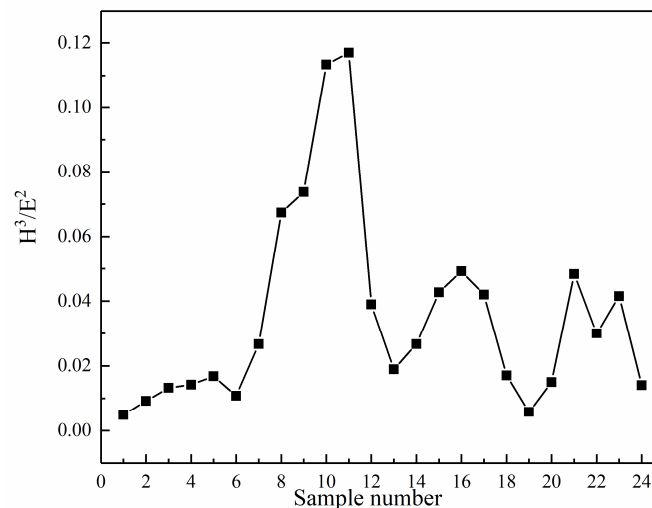


Figure 3. Ratio of hardness to elastic modulus (H^3/E^2) of HEA coatings with different parameters.

The friction and wear tests of HEA coatings were performed using a UMT-Tribolab tribometer (Bruker, Saarbrücken, Germany), shown in Figure 4. The grinding ball was Si₃N₄ with a diameter of 6 mm, a load of 5 N, a wear scar length of 5 mm, a sliding frequency of 4 Hz, and a wear time of 30 min. The experimental parameters of friction and wear in a drilling fluid environment (wet) were consistent with those of the dry friction and wear experiment (dry) except for the different environment. The drilling fluid was composed of 5% KCl, 4% bentonite, 0.25% Na₂CO₃, and 0.5% xanthan gum (wt.%) with pH value of 9. The wear experiment was repeated three times under each experimental parameter. The coating wear rate was calculated according to the formula $Q = \frac{V_W}{NS}$, where Q is the wear rate (mm³·N⁻¹·m⁻¹), V_W is the wear volume (mm³), N is the applied load (N), and S is the total sliding distance (m) [33]. N and S are determined. V_W can be obtained by multiplying the cross-sectional area of the wear scar by the length of the wear scar. The cross-sectional area of the wear scar can be measured by a 3D white light interferometer (NeXView, ZYGO, Middlefield, CT, USA), but there must be some error. In order to minimize the error, the average cross-sectional area of the three positions of the wear scars was used as the average cross-sectional area, and the average cross-sectional area was multiplied by the length of the wear scars to obtain the wear rate of the coating. Therefore, the friction and wear experiments of 24 kinds of HEA coatings with different parameters were carried out three times in two different environments (dry sliding wear or wet sliding wear); thus,

144 groups of wear data were obtained. The HEA coatings with different parameters were numbered, and the sample numbers of HEA coatings are shown in Table 1. The wear rates of HEA coatings with different parameters are shown in Figure 5. The wear resistance of the coating is closely related to the wear rate. The lower the wear rate of HEA coatings, the better the wear resistance.

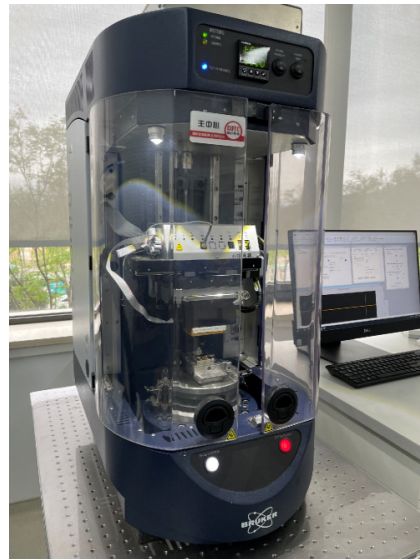


Figure 4. The experiment on the UMT-Tribo-lab tribometer.

Table 1. Sample numbers of HEA coatings with different parameters.

Sample Number	Mixture Powder	VHT (°C)	Wear Form
S1	1	Untreated	Dry
S2	2	Untreated	Dry
S3	3	Untreated	Dry
S4	4	Untreated	Dry
S5	5	Untreated	Dry
S6	6	Untreated	Dry
S7	1	500	Dry
S8	2	500	Dry
S9	3	500	Dry
S10	4	500	Dry
S11	5	500	Dry
S12	6	500	Dry
S13	1	700	Dry
S14	2	700	Dry
S15	3	700	Dry
S16	4	700	Dry
S17	5	700	Dry
S18	6	700	Dry
S19	1	900	Dry
S20	2	900	Dry
S21	3	900	Dry
S22	4	900	Dry
S23	5	900	Dry
S24	6	900	Dry
S25	1	Untreated	Wet
S26	2	Untreated	Wet
S27	3	Untreated	Wet
S28	4	Untreated	Wet

Table 1. Cont.

Sample Number	Mixture Powder	VHT (°C)	Wear Form
S29	5	Untreated	Wet
S30	6	Untreated	Wet
S31	1	500	Wet
S32	2	500	Wet
S33	3	500	Wet
S34	4	500	Wet
S35	5	500	Wet
S36	6	500	Wet
S37	1	700	Wet
S38	2	700	Wet
S39	3	700	Wet
S40	4	700	Wet
S41	5	700	Wet
S42	6	700	Wet
S43	1	900	Wet
S44	2	900	Wet
S45	3	900	Wet
S46	4	900	Wet
S47	5	900	Wet
S48	6	900	Wet

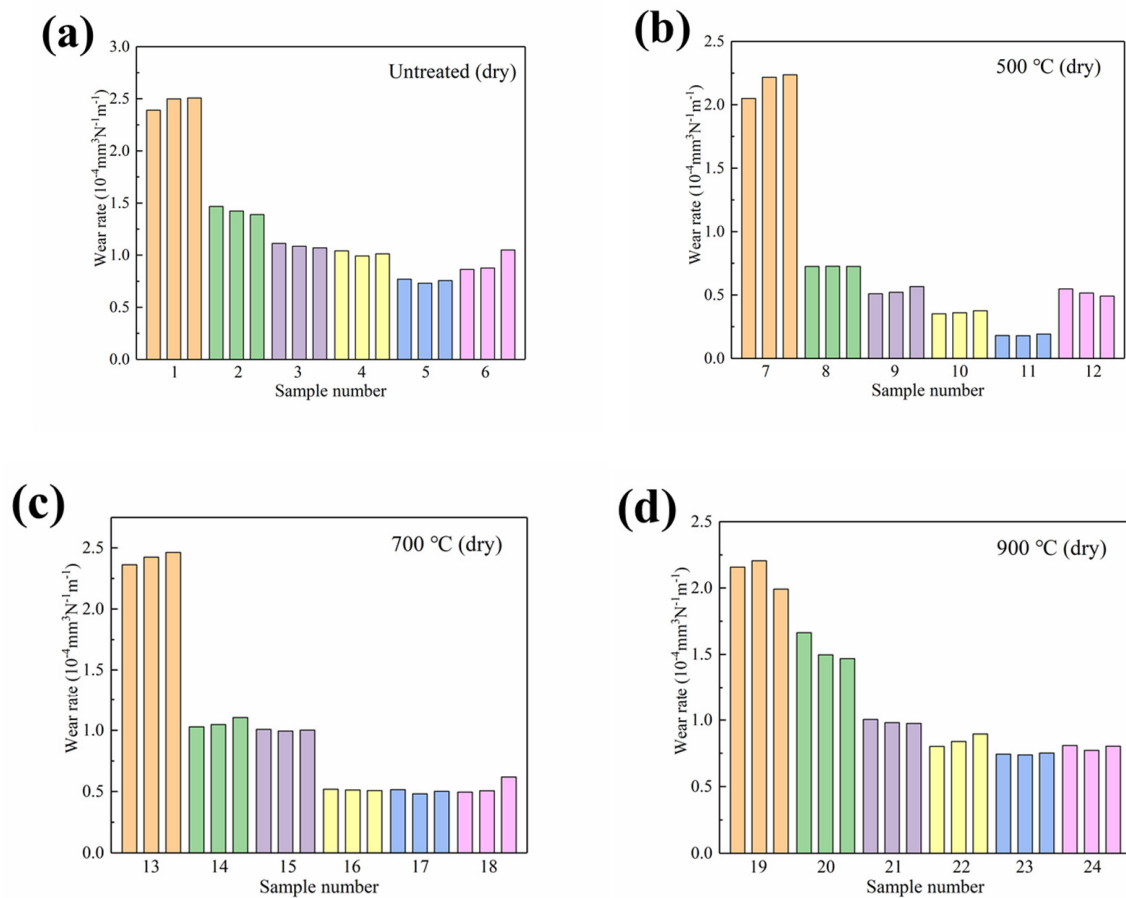


Figure 5. Cont.

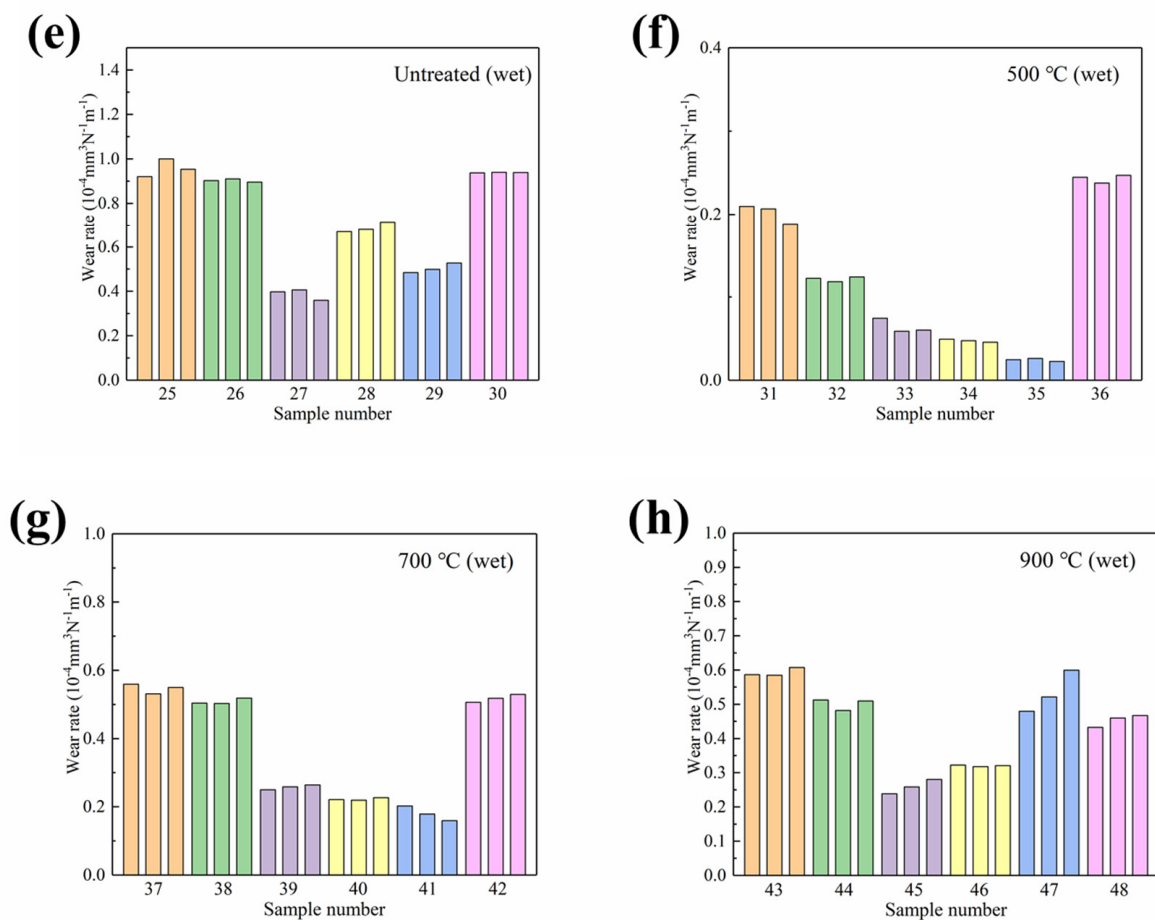


Figure 5. Wear rates of HEA coatings with different parameters. (a) Untreated (dry); (b) 500 °C (dry); (c) 700 °C (dry); (d) 900 °C (dry); (e) Untreated (wet); (f) 500 °C (wet); (g) 700 °C (wet); and (h) 900 °C (wet).

2.2. Machine Learning Models

The coating composition (different contents of Al, Ti, and Cu elements), H^3/E^2 , VHT temperature (500, 700, and 900 °C) and wear form (dry sliding wear or wet sliding wear) were used as input variables, and the wear rates of HEA coatings with different parameters were used as output variables. To test the model used to predict the wear rate of AlCoCrFeNi-X (Ti, Cu) HEA coatings, the dataset was divided into two parts: the training dataset and the test dataset. The training dataset included 126 samples (87.5% of all data) and the test dataset included 18 samples (12.5% of all data). Training and predicting wear rates by using the scikit-learn (0.24.2) algorithm database in Python 3.9. Four machine learning algorithms were used to model the test dataset: CART, RF, GBDT, and AdaBoost. The introduction of the four machine learning algorithms is as follows:

The CART model is a kind of decision tree, and it can be used to create classification trees and regression trees. This algorithm uses the Gini index based on the minimum distance to estimate the function, with high computational efficiency. The CART algorithm can allow partial misclassification and appears very robust in the face of problems such as missing values and many variables. When the dataset is small, this algorithm often has high prediction accuracy, but it is prone to overfitting.

The RF model is an integrated learning algorithm based on trees. It is an integrated technique to obtain final prediction results from multiple decision trees, and it can be used for classification and regression tasks. The basic principle of the RF algorithm is as follows: Samples from the training set are randomly selected to build a decision tree. Then, repeating the process, multiple trees are built, and, finally, the results of each tree

are aggregated as the final forecast. The advantage of the RF algorithm is that it can make good use of the existing data, can extract useful information from the data, and has high accuracy. It can deal with a large number of features effectively and has a certain degree of fault tolerance [34].

The GBDT model is a gradient boosting decision tree algorithm, developed rapidly in machine learning algorithms in recent years. This algorithm uses the weak learning algorithm to construct a strong learning model several times iteratively. It is an integrated algorithm composed of multiple weak learners. The basic idea of the GBDT algorithm is to combine the results of multiple weak learners to improve the prediction accuracy of the classifier. The GBDT algorithm is an iterative algorithm; each iteration will build a decision tree, and each tree will be built based on the error of the last tree, so as to build a stronger set of decision trees and provide more accurate results [35].

The AdaBoost model is an iterative algorithm that uses a series of weak classifiers to build a strong classifier and effectively converts the learning task into an optimization problem. The basic principle of the AdaBoost algorithm is to allow weak classifiers to better fit the data, thus improving the accuracy of classification. The AdaBoost algorithm is simple, easy to implement, and can solve most classification problems. In addition, AdaBoost algorithm has high accuracy and does not easily overfit. Therefore, the AdaBoost algorithm can effectively solve the classification problem in machine learning [36].

The differences and connections between these four machine learning algorithms are as follows: CART is a binary recursive segmentation technology that is an implementation of a decision tree. It can be used for both classification tasks and regression tasks [37]. In view of the data characteristics of this study, this algorithm was used to solve the regression problem. The CART algorithm is a nonparametric method suitable for modeling with small amounts of data and does not require prior assumptions about the relationship between input variables. It mainly trains the model from the dataset. The other three algorithms (RF, GBDT, and AdaBoost) are all derived and extended from this algorithm. RF is an integration algorithm based on bagging that integrates multiple decision trees to train and predict samples. Bagging can be simply understood as randomly sampling from the dataset with replacement. Both GBDT and AdaBoost are boosting algorithms; that is, each calculation is carried out to reduce the residual error of the previous one, strengthening the weak decision tree continuously until the desired effect is achieved [38]. AdaBoost uses misfraction data points to identify problems and improves the model by adjusting the weight of misfraction data points. GBDT identifies problems through negative gradients and improves the model by calculating negative gradients [39]. For a specific dataset, it is incorrect to state that the more complex the algorithm, the better the prediction effect. Therefore, these four machine learning algorithms were selected and their application effects are discussed.

2.3. Model Performance and Feature Importance

The error between the predictive values using different machine learning algorithms and the experimental values was analyzed in order to estimate the measurement uncertainty of the obtained results. Aiming at the problem of overfitting of the algorithm, 10-k cross-validation was used for verification to maximize the generalization ability of the model. Multiple evaluation indicators were used to evaluate the prediction accuracy of machine learning models, including the mean absolute error (MAE), root-mean-square error (RMSE), and R-squared (R^2). An optimized model for predicting the wear-resistant AlCoCrFeNi-X (Ti, Cu) HEA coatings for drilling equipment was obtained. The feature importance of each input variable was analyzed to evaluate the influence of different factors on the wear rate of HEA coatings.

3. Results and Discussion

The experimental values and predictive values from different machine learning algorithms are shown in Figure 6. It can be seen that the four machine learning algorithms

were able to predict the wear rates of HEA coatings to a certain extent. The predictive values from CART, RF, and AdaBoost are basically consistent with the experimental values; therefore, these algorithms have higher prediction accuracy. Furthermore, GBDT has high discreteness of individual data.

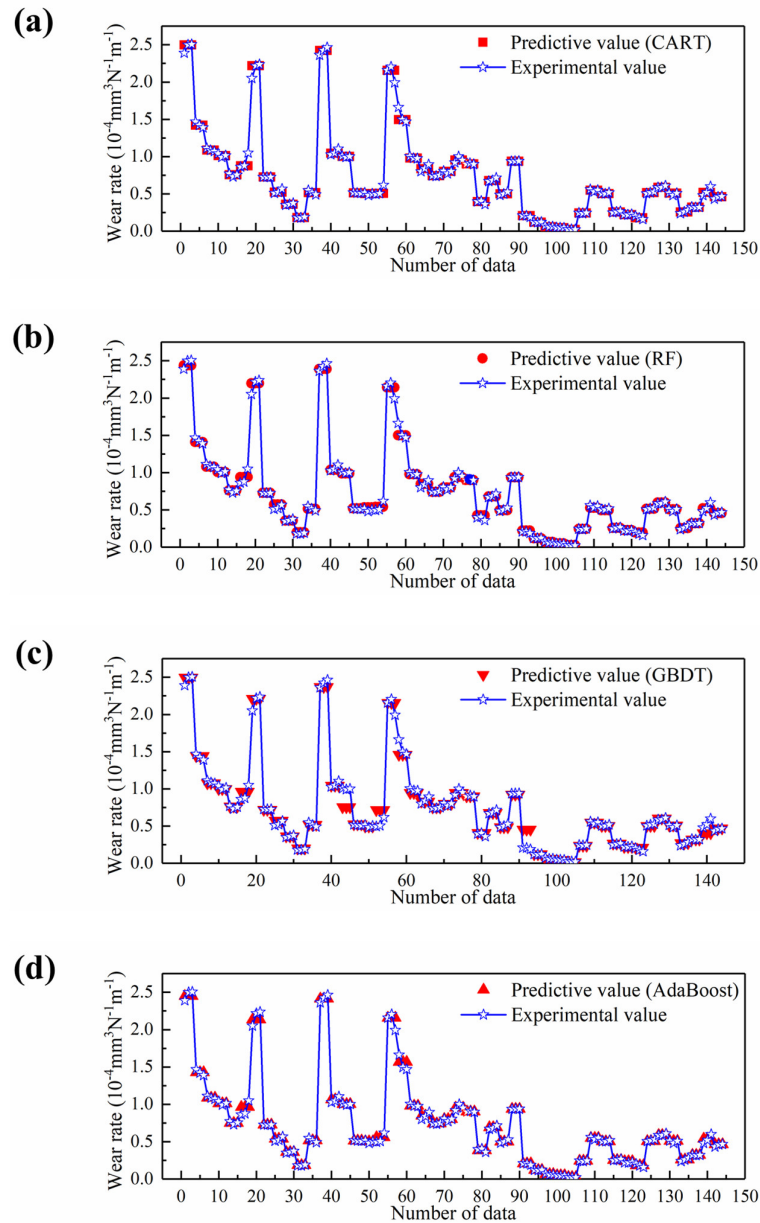


Figure 6. Experimental and predictive values from different machine learning algorithms. (a) CART; (b) RF; (c) GBDT; and (d) AdaBoost.

The errors between the predictive values using different machine learning algorithms and the experimental values are shown in Figure 7. The error of the CART model is mainly concentrated within -0.2 to 0.1 , and that of RF is mainly concentrated within -0.2 to 0.4 . Part of the error of the GBDT model is large, with five groups of data exceeding ± 0.5 , and the rest are mainly concentrated within -0.3 to 0.4 . The error of the AdaBoost model is mostly concentrated within -0.1 to 0.1 , among which the error of three groups of data is more than ± 1.0 . Because the AdaBoost algorithm is sensitive to outliers, the prediction effect may not be very good when there is an order of magnitude difference in the dataset.

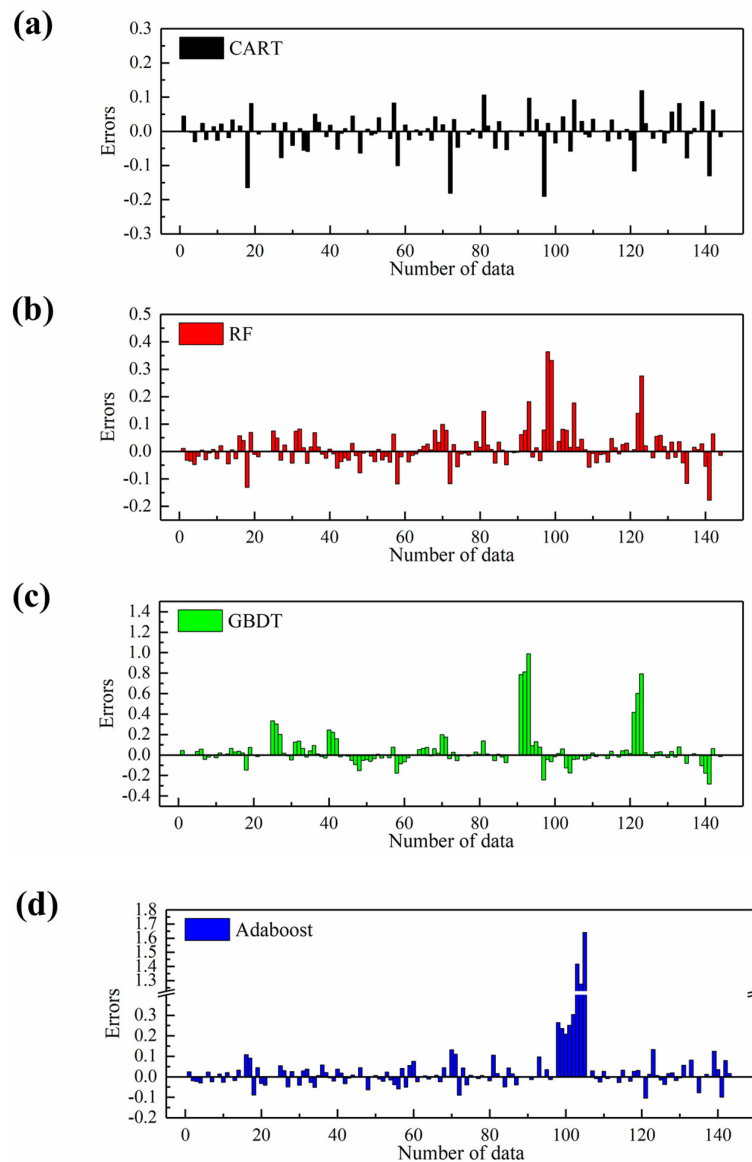


Figure 7. Errors from different machine learning algorithms. (a) CART; (b) RF; (c) GBDT; and (d) AdaBoost.

It is easy to overfit the data in the growth process of the decision tree; therefore, 10-k cross-validation was used for verification to maximize the generalization ability of the model [40]. All data were used as test and training datasets for 10-k cross-validation, and the accuracy of the four machine learning models was further tested using multiple evaluation indicators. MAE is the average value of the absolute error, which is used to evaluate the closeness between the prediction results and the real dataset. MAE can reflect the actual situation of predicted error; the smaller the MAE value, the better the model fitting effect. The equation is as follows [29]:

$$\text{MAE} = \frac{1}{N} \sum_{i=1}^N |\hat{y}_i - y_i| \quad (1)$$

RMSE is the square root of the ratio of the square sum of the deviation between the observed value, the true value, and the observation number, which is used to measure

the deviation between the observed value and the true value. RMSE is more sensitive to outliers. The equation is as follows [29]:

$$RMSE = \sqrt{\frac{1}{N} \sum_{i=1}^N (\hat{y}_i - y_i)^2} \tag{2}$$

R^2 is an effective indicator to measure the prediction ability of the regression model, which can accurately reflect the accuracy of the prediction degree of the regression model. This index often needs to be combined with other indicators to evaluate the fitting degree of the regression model. The formula is as follows [29]:

$$R^2 = 1 - \frac{\sum (y_i - \hat{y}_i)^2}{\sum (y_i - \bar{y})^2} \tag{3}$$

In the above four formulas, y_i represents the actual value, \hat{y}_i represents the predicted value, and \bar{y} represents the mean of all actual values. The evaluation indicators of different machine learning models and the results of evaluation indicators are shown in Figure 8 and Table 2. The average MAE of the four models (CART, RT, GBDT, and AdaBoost) is 3.3%, 5.0%, 7.2%, and 3.4%, respectively, and CART has the smallest MAE value. The average RMSE is 5.7%, 8.0%, 9.7%, and 5.7%. The smaller the RMSE, the higher the prediction accuracy of the model. The average values of MAPE are 4.4%, 10.0%, 18.9%, and 8.5% and the average values of R^2 are 99.0%, 98.0%, 94.0%, and 98.7%, respectively. The closer R^2 is to 1, the higher the prediction accuracy of the model. A comprehensive analysis of several evaluation indicators shows that all models achieved good results except for the GBDT model, which also proves the reliability of the decision tree model for predicting the wear rate of AlCoCrFeNi-X (Ti, Cu) HEA coatings. Because of the small amount of data, the CART model had the best prediction performance and can provide guidance for predicting the wear resistance of AlCoCrFeNi-X (Ti, Cu) HEA coatings for drilling equipment.

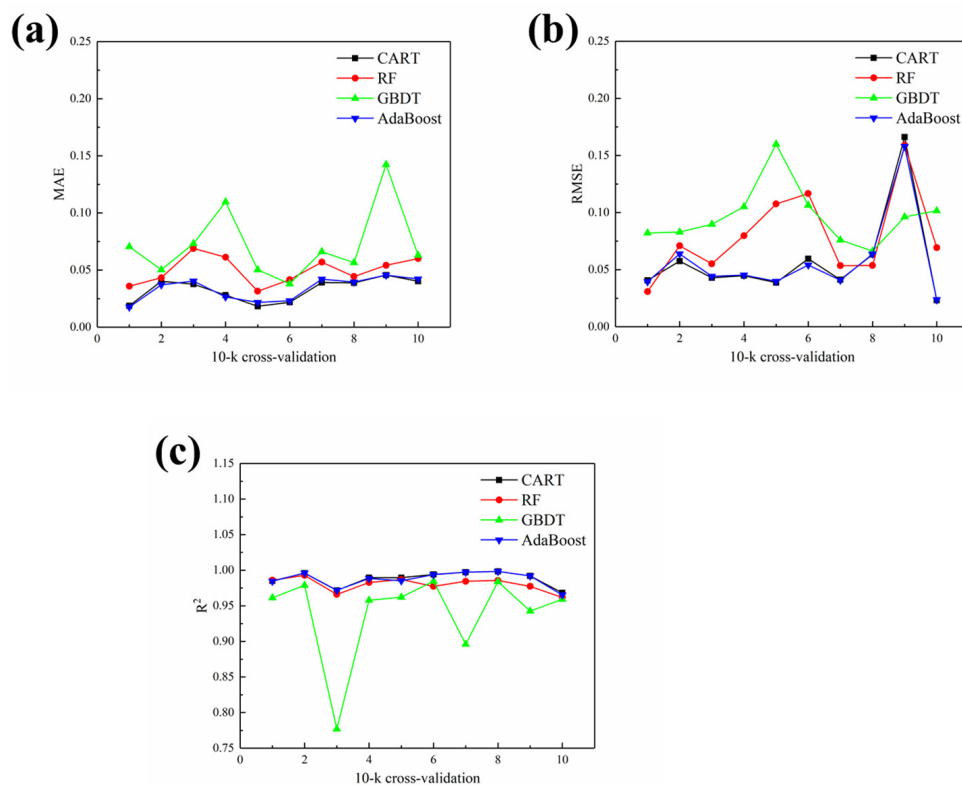
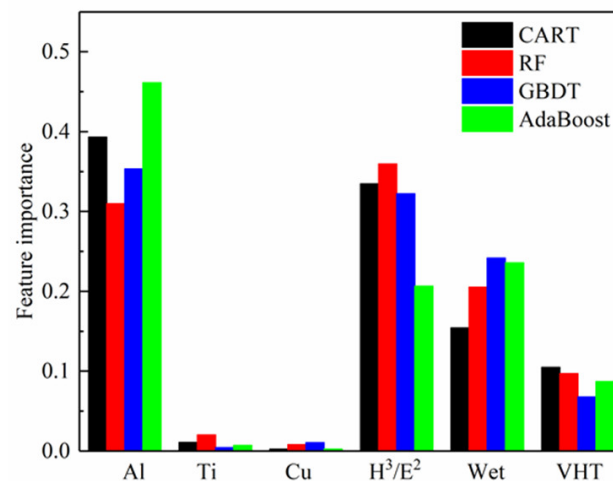


Figure 8. Evaluation indicators of different machine learning models. (a) MAE; (b) RMSE; and (c) R^2 .

Table 2. The results of evaluation indicators of different machine learning models.

Model	MAE	RMSE	R ²
CART	3.3%	5.7%	99.0%
RF	5.0%	8.0%	98.0%
GBDT	7.2%	9.7%	94.0%
AdaBoost	3.4%	5.7%	98.7%

Different input variables in the dataset have different effects on wear resistance of AlCoCrFeNi-X (Ti, Cu) HEA coatings; therefore, the feature importance of input variables affecting wear rates in the four models was evaluated separately, as shown in Figure 9. Some variables are prominent, such as the Al element and addition amount. This phenomenon is more obvious in AdaBoost. The addition of Al causes lattice distortion; with an increase in the amount of added Al, lattice distortion is further intensified and the strength of the coating improves [41]. The second is the wear form. The friction and wear failure mechanism of HEA coatings under different environments (dry sliding wear or wet sliding wear) are different. Drilling fluid not only plays a corrosive role in wear, but also plays a lubricating role. The third is H^3/E^2 ; this data point can reflect the elastic strain and resistance to plastic deformation of the coating. As a result, H^3/E^2 is closely related to wear resistance. The fourth is the VHT temperature. VHT temperature affects the hardness and elastic modulus of the coating, but the relationship between VHT temperature and these factors is not linear. The addition of Ti and Cu in machine learning has the least effect on wear rates of HEA coatings. It is worth noting that the addition of Ti and Cu elements does not have zero effect on the wear resistance of AlCoCrFeNi-X (Ti, Cu) HEA coatings, but it has less impact on the wear rate compared with other influencing factors.

**Figure 9.** Feature importance of input variables.

It should be explained that there are some limitations in this study. First, for the possible overfitting problem, we adopted the 10-k cross-validation method and solved this problem well. Secondly, in terms of input variable determination, the addition of Ti and Cu elements had no significant effect on the wear rate of AlCoCrFeNi-X (Ti, Cu) HEA coatings. This may be due to the fact that the addition of Ti or Cu also affects the content of Al, so the relationship between these elements is not completely nonlinear. Thirdly, the amount of data was limited by the experimental conditions. For example, only six different compositions of powders were designed for HVOF spraying. In the future, the amount of data will be further expanded to further improve the prediction accuracy of the machine learning model.

4. Conclusions

(1) The coating composition (different contents of Al, Ti, and Cu elements), ratio of hardness and elastic modulus (H^3/E^2), VHT temperature (500, 700, and 900 °C), and wear form (dry or wet) were used as input variables, and the wear rates of AlCoCrFeNi-X (Ti, Cu) HEA coatings were used as output variables. The dataset was obtained entirely by experiment. Four machine learning algorithms (CART, RF, GBDT, and AdaBoost) were used to predict the wear resistance of HEA coatings based on a small amount of data.

(2) All models demonstrated good performance except for the GBDT model, which also proves the reliability of the decision tree model for predicting the wear rate of AlCoCrFeNi-X (Ti, Cu) HEA coatings. Because of the small amount of data, the CART model demonstrated the best prediction performance. After the use of 10-k cross-validation, the average MAE, RMSE, and R^2 values of the CART model were 3.3%, 5.7%, and 99.0%, respectively. The CART model can provide guidance for predicting the wear resistance of AlCoCrFeNi-X (Ti, Cu) HEA coatings for drilling equipment.

(3) By analyzing the feature importance of input variables, the contribution of different factors to the wear rate of AlCoCrFeNi-X (Ti, Cu) HEA coatings was obtained. Al content had the greatest influence on wear rate, followed by H^3/E^2 , wear form, and VHT temperature. The addition of Ti and Cu had no significant effect on the wear rate of AlCoCrFeNi-X (Ti, Cu) HEA coatings.

Author Contributions: Conceptualization, J.K., Y.Z. and Y.F.; Methodology, J.K., Y.N., Y.Z. and G.M.; Software, Y.N.; Validation, Y.Z.; Formal analysis, J.K. and Y.Z.; Resources, Y.F. and G.M.; Data curation, Y.N., Y.F. and G.M.; Writing—original draft, J.K.; Writing—review & editing, Y.Z.; Project administration, J.K. and G.M.; Funding acquisition, J.K. and G.M. All authors have read and agreed to the published version of the manuscript.

Funding: This research was funded by the National Key R&D Program of China (2022YFB3706600), the National Natural Science Foundation of China (52175196, 52275218), and the Fundamental Research Funds for Central Universities (265QZZ2021008).

Data Availability Statement: Data presented in this article are available at request from the corresponding author.

Conflicts of Interest: The authors declare no conflict of interest.

References

1. Lin, L.; Li, G.L.; Wang, H.D.; Kang, J.J.; Xu, Z.L.; Wang, H.J. Structure and Wear Behavior of NiCr–Cr₃C₂ Coatings Sprayed by Supersonic Plasma Spraying and High Velocity Oxy-Fuel Technologies. *Appl. Surf. Sci.* **2015**, *356*, 383–390. [[CrossRef](#)]
2. Zhu, L.N.; Wang, C.B.; Wang, H.D.; Xu, B.S.; Zhuang, D.M.; Liu, J.J.; Li, G.L. Microstructure and Tribological Properties of WS₂/MoS₂ Multilayer Films. *Appl. Surf. Sci.* **2012**, *258*, 1944–1948. [[CrossRef](#)]
3. Menghani, J.; Vyas, A.; Patel, P.; Natu, H.; More, S. Wear, Erosion and Corrosion Behavior of Laser Cladded High Entropy Alloy Coatings—A Review. *Mater. Today Proc.* **2021**, *38*, 2824–2829. [[CrossRef](#)]
4. Yeh, J.W.; Chen, S.K.; Lin, S.J.; Gan, J.Y.; Chin, T.S.; Shun, T.T.; Tsau, C.H.; Chang, S.Y. Nanostructured High-Entropy Alloys with Multiple Principal Elements: Novel Alloy Design Concepts and Outcomes. *Adv. Eng. Mater.* **2004**, *6*, 299–303. [[CrossRef](#)]
5. Cantor, B.; Chang, I.T.H.; Knight, P.; Vincent, A.J.B. Microstructural Development in Equiatomic Multicomponent Alloys. *Mater. Sci. Eng. A* **2004**, *375–377*, 213–218. [[CrossRef](#)]
6. Tokarewicz, M.; Grądzka-Dahlke, M. Review of Recent Research on AlCoCrFeNi High-Entropy Alloy. *Metals* **2021**, *11*, 1302. [[CrossRef](#)]
7. Li, W.D.; Xie, D.; Li, D.Y.; Zhang, Y.; Gao, Y.F.; Liaw, P.K. Mechanical Behavior of High-Entropy Alloys. *Prog. Mater. Sci.* **2021**, *118*, 100777. [[CrossRef](#)]
8. Varalakshmi, S.; Appa Rao, G.; Kamaraj, M.; Murty, B.S. Hot Consolidation and Mechanical Properties of Nanocrystalline Equiatomic AlFeTiCrZnCu High Entropy Alloy after Mechanical Alloying. *J. Mater. Sci.* **2010**, *45*, 5158–5163. [[CrossRef](#)]
9. Luo, H.; Li, Z.M.; Mingers, A.M.; Raabe, D. Corrosion Behavior of an Equiatomic CoCrFeMnNi High-Entropy Alloy Compared with 304 Stainless Steel in Sulfuric Acid Solution. *Corros. Sci.* **2018**, *134*, 131–139. [[CrossRef](#)]
10. Oses, C.; Toher, C.; Curtarolo, S. High-Entropy Ceramics. *Nat. Rev. Mater.* **2020**, *5*, 295–309. [[CrossRef](#)]
11. Asadikiya, M.; Yang, S.; Zhang, Y.; Lemay, C.; Apelian, D.; Zhong, Y. A Review of the Design of High-Entropy Aluminum Alloys: A Pathway for Novel Al Alloys. *J. Mater. Sci.* **2021**, *56*, 12093–12110. [[CrossRef](#)]

12. Komarasamy, M.; Kumar, N.; Mishra, R.S.; Liaw, P.K. Anomalies in the Deformation Mechanism and Kinetics of Coarse-Grained High Entropy Alloy. *Mater. Sci. Eng. A* **2016**, *654*, 256–263. [[CrossRef](#)]
13. Ji, X.; Alavi, S.H.; Harimkar, S.P.; Zhang, Y. Sliding Wear of Spark Plasma Sintered CrFeCoNiCu High-Entropy Alloy Coatings: Effect of Aluminum Addition. *J. Materi. Eng. Perform.* **2018**, *27*, 5815–5822. [[CrossRef](#)]
14. Wu, M.Y.; Yuan, J.F.; Diao, G.J.; Li, D.Y. Achieving a Combination of Higher Strength and Higher Ductility for Enhanced Wear Resistance of AlCrFeNiTi_{0.5} High-Entropy Alloy by Mo Addition. *Metals* **2022**, *12*, 1910. [[CrossRef](#)]
15. Prabu, G.; Duraiselvam, M.; Jeyaprakash, N.; Yang, C.-H. Microstructural Evolution and Wear Behavior of AlCoCrCuFeNi High Entropy Alloy on Ti–6Al–4V Through Laser Surface Alloying. *Met. Mater. Int.* **2021**, *27*, 2328–2340. [[CrossRef](#)]
16. Zhou, Y.K.; Kang, J.J.; Zhang, J.; Zhu, S.; Fu, Z.Q.; Zhu, L.N.; She, D.S. Effect of Nitriding on Microstructure and Wear Behavior of HVOF Sprayed Al_xCoCrFeNi (X = 0.4, 0.7, 1.0) High-Entropy Alloy Coatings. *Intermetallics* **2022**, *151*, 107709. [[CrossRef](#)]
17. Meghwal, A.; Anupam, A.; Schulz, C.; Hall, C.; Murty, B.S.; Kottada, R.S.; Vijay, R.; Munroe, P.; Berndt, C.C.; Ang, A.S.M. Tribological and Corrosion Performance of an Atmospheric Plasma Sprayed AlCoCr_{0.5}Ni High-Entropy Alloy Coating. *Wear* **2022**, *506–507*, 204443. [[CrossRef](#)]
18. Liu, H.; Liu, J.; Li, X.; Chen, P.J.; Yang, H.F.; Hao, J.B. Effect of Heat Treatment on Phase Stability and Wear Behavior of Laser Clad AlCoCrFeNiTi_{0.8} High-Entropy Alloy Coatings. *Surf. Coat. Technol.* **2020**, *392*, 125758. [[CrossRef](#)]
19. Peng, Q.Q.; Liu, M.; Huang, Y.F.; Zhou, X.Y.; Ma, G.Z.; Wang, H.D.; Xing, Z.G. Effect of Heat Treatment on Microstructure and Properties of Al-25Si Wear-Resistant Coatings Sprayed by Supersonic Plasma. *J. Therm. Spray Tech.* **2022**. [[CrossRef](#)]
20. Sun, J.; Dai, S.C.; Zhang, D.B.; Si, W.D.; Jiang, B.C.; Shu, D.; Wu, L.L.; Zhang, C.; Zhang, M.S.; Xiong, X.Y. Friction and Wear Properties of CoCrFeNiMnSn_x High Entropy Alloy Coatings Prepared via Laser Cladding. *Metals* **2022**, *12*, 1230. [[CrossRef](#)]
21. Silvello, A.; Diaz, E.T.; Ramirez, E.R.; Cano, I.G. Microstructural, Mechanical and Wear Properties of Atmospheric Plasma-Sprayed and High-Velocity Oxy-Fuel AlCoCrFeNi Equiatomic High-Entropy Alloys (HEAs) Coatings. *J. Therm. Spray Tech.* **2023**, *32*, 425–442. [[CrossRef](#)]
22. Zhang, D.D.; He, X.Y.; Gao, Y.L.; Qin, B.L. Investigation of the Microstructure and Wear Properties of Laser Clad Al-Si Coatings Containing Different Y₂O₃ Contents. *Coatings* **2023**, *13*, 308. [[CrossRef](#)]
23. Martins, P.S.; Pires, S.S.; da Silva, E.R.; Vieira, V.F.; Ba, E.C.T.; Dias, C.A.R. Tribological aspects of the Diamond-like carbon film applied to different surfaces of AISI M2 steel. *Wear* **2022**, *506–507*, 204469. [[CrossRef](#)]
24. Hsu, C.H.; Lin, C.Y.; You, W.S. Microstructure and Dry/Wet Tribological Behaviors of 1% Cu-Alloyed Austempered Ductile Iron. *Materials* **2023**, *16*, 2284. [[CrossRef](#)]
25. Çetinel, H.; Öztürk, H.; Çelik, E.; Karlık, B. Artificial Neural Network-Based Prediction Technique for Wear Loss Quantities in Mo Coatings. *Wear* **2006**, *261*, 1064–1068. [[CrossRef](#)]
26. Zhou, R.Z.; Xing, Z.G.; Wang, H.D.; Piao, Z.Y.; Huang, Y.F.; Guo, W.L.; Ma, R.B. Prediction of Contact Fatigue Life of AT40 Ceramic Coating Based on Neural Network. *Anti-Corros. Methods Mater.* **2020**, *67*, 83–100. [[CrossRef](#)]
27. Hasan, M.S.; Kordijazi, A.; Rohatgi, P.K.; Nosonovsky, M. Triboinformatics Approach for Friction and Wear Prediction of Al-Graphite Composites Using Machine Learning Methods. *J. Tribol.* **2021**, *144*, 011701. [[CrossRef](#)]
28. Li, Y.G.; Liu, C.Q.; Hua, J.Q.; Gao, J.; Maropoulos, P. A Novel Method for Accurately Monitoring and Predicting Tool Wear under Varying Cutting Conditions Based on Meta-Learning. *CIRP Ann. Manuf. Technol.* **2019**, *68*, 487–490. [[CrossRef](#)]
29. Ulas, M.; Altay, O.; Gurgenc, T.; Özel, C. A New Approach for Prediction of the Wear Loss of PTA Surface Coatings Using Artificial Neural Network and Basic, Kernel-Based, and Weighted Extreme Learning Machine. *Friction* **2020**, *8*, 1102–1116. [[CrossRef](#)]
30. Altay, O.; Gurgenc, T.; Ulas, M.; Özel, C. Prediction of Wear Loss Quantities of Ferro-Alloy Coating Using Different Machine Learning Algorithms. *Friction* **2020**, *8*, 107–114. [[CrossRef](#)]
31. Mojena, M.A.R.; Roca, A.S.; Zamora, R.S.; Orozco, M.S.; Fals, H.C.; Lima, C.R.C. Neural Network Analysis for Erosive Wear of Hard Coatings Deposited by Thermal Spray: Influence of Microstructure and Mechanical Properties. *Wear* **2017**, *376–377*, 557–565. [[CrossRef](#)]
32. Wen, S.P.; Zong, R.L.; Zeng, F.; Guo, S.; Pan, F. Nanoindentation and Nanoscratch Behaviors of Ag/Ni Multilayers. *Appl. Surf. Sci.* **2009**, *255*, 4558–4562. [[CrossRef](#)]
33. Miao, J.W.; Liang, H.; Zhang, A.J.; He, J.Y.; Meng, J.H.; Lu, Y.P. Tribological Behavior of an AlCoCrFeNi_{2.1} Eutectic High Entropy Alloy Sliding Against Different Counterfaces. *Tribol. Int.* **2021**, *153*, 106599. [[CrossRef](#)]
34. Schonlau, M.; Zou, R.Y. The Random Forest Algorithm for Statistical Learning. *Stata J.* **2020**, *20*, 3–29. [[CrossRef](#)]
35. Liang, W.Z.; Luo, S.Z.; Zhao, G.Y.; Wu, H. Predicting Hard Rock Pillar Stability Using GBDT, XGBoost, and LightGBM Algorithms. *Mathematics* **2020**, *8*, 765. [[CrossRef](#)]
36. Wen, X.Z.; Shao, L.; Xue, Y.; Fang, W. A Rapid Learning Algorithm for Vehicle Classification. *Inf. Sci.* **2015**, *295*, 395–406. [[CrossRef](#)]
37. Li, Y. Predicting Materials Properties and Behavior Using Classification and Regression Trees. *Mater. Sci. Eng. A* **2006**, *433*, 261–268. [[CrossRef](#)]
38. Niu, Y.; Li, Z.M.; Fan, Y.X. Analysis of Truck Drivers' Unsafe Driving Behaviors Using Four Machine Learning Methods. *Int. J. Ind. Ergon.* **2021**, *86*, 103192. [[CrossRef](#)]
39. Nait Amar, M.; Shateri, M.; Hemmati-Sarapardeh, A.; Alamatsaz, A. Modeling Oil-Brine Interfacial Tension at High Pressure and High Salinity Conditions. *J. Pet. Sci. Eng.* **2019**, *183*, 106413. [[CrossRef](#)]

40. Chen, S.; Kaufmann, T. Development of Data-Driven Machine Learning Models for the Prediction of Casting Surface Defects. *Metals* **2021**, *12*, 1. [[CrossRef](#)]
41. Joseph, J.; Haghdad, N.; Shamlaye, K.; Hodgson, P.; Barnett, M.; Fabijanic, D. The Sliding Wear Behaviour of CoCrFeMnNi and Al_xCoCrFeNi High Entropy Alloys at Elevated Temperatures. *Wear* **2019**, *428–429*, 32–44. [[CrossRef](#)]

Disclaimer/Publisher's Note: The statements, opinions and data contained in all publications are solely those of the individual author(s) and contributor(s) and not of MDPI and/or the editor(s). MDPI and/or the editor(s) disclaim responsibility for any injury to people or property resulting from any ideas, methods, instructions or products referred to in the content.